Optical Power of the Isolated Human Crystalline Lens

David Borja,[1,2] *Fabrice Manns,*[1,2] *Arthur Ho,*[3,4,5] *Noel Ziebarth,*[1,2] *Alexandre M. Rosen,*[1,2] *Rakhi Jain,*[6] *Adriana Amelinckx,*[1] *Esdras Arrieta,*[1] *Robert C. Augusteyn,*[5,7] *and Jean-Marie Parel*[1,2,5,8]

PURPOSE. To characterize the age dependence of isolated human crystalline lens power and quantify the contributions of the lens surfaces and refractive index gradient.

METHODS. Experiments were performed on 100 eyes of 73 donors (average 2.8 ± 1.6 days postmortem) with an age range of 6 to 94 years. Lens power was measured with a modified commercial lensmeter or with an optical system based on the Scheiner principle. The radius of curvature and asphericity of the isolated lens surfaces were measured by shadow photography. For each lens, the contributions of the surfaces and the refractive index gradient to the measured lens power were calculated by using optical ray-tracing software. The age dependency of these refractive powers was assessed.

RESULTS. The total refractive power and surface refractive power both showed a biphasic age dependency. The total power decreased at a rate of -0.41 D/y between ages 6 and 58.1, and increased at a rate of 0.33D/y between ages 58.1 and 82. The surface contribution decreased at a rate of -0.13 D/y between ages 6 and 55.2 and increased at a rate of 0.04 D/y between ages 55.2 and 94. The relative contribution of the surfaces increased by 0.17% per year. The equivalent refractive index also showed a biphasic age dependency with a decrease at a rate of -3.9×10^{-4} per year from ages 6 to 60.4 followed by a plateau.

CONCLUSIONS. The lens power decreases with age, due mainly to a decrease in the contribution of the gradient. The use of a constant equivalent refractive index value to calculate lens power with the lens maker formula will underestimate the power of young lenses and overestimate the power of older lenses. (*Invest Ophthalmol Vis Sci.* 2008;49:2541–2548) DOI: 10.1167/iovs.07-1385

The optical power of the crystalline lens is determined by the surface curvatures, the refractive index differences at the aqueous lens and lens vitreous interfaces, and the refractive index gradient distribution within the lens.[1] Studying the optical properties of the lens (i.e., optical power, refractive index distribution, and the surface refractive contributions) in vivo is difficult because of the position of the lens behind the cornea and pupil, as well as the distortions of the posterior lens surface caused by the lens refractive index gradient. Two approaches have been used to measure the lens power in vivo. In the first approach the curvatures of the lens surface and lens thickness are measured by phakometry and ultrasonic or optical biometry. The lens power is then calculated assuming an equivalent uniform refractive index (typically, $\sim$1.42).[2,3] In the second approach, the lens power is calculated from measurements of axial eye length, anterior chamber depth, corneal power, and refractive state of the eye. These parameters are input into an eye model to calculate the power required for the lens to produce an optical system that matches the measurements.[3–6] Both techniques derive the lens power from measurements of other ocular parameters. Even though recent studies have cross-validated in vivo lens biometry techniques[7,8] some assumptions are necessary either for the refractive index of the lens, or for the parameters of the eye model.

Direct measurements of the lens power (or focal length) can be obtained on in vitro lenses.[9–15] A comparison of in vivo[16] and in vitro[17] lens shape and power suggests that the isolated lens, which is free of zonular tension, assumes a shape and power similar to those of the maximally accommodated lens in vivo. Measuring the shape and power of isolated lenses can therefore provide information on the optical changes occurring in the maximally accommodated lens with age, as long as special care is taken to avoid swelling and other changes caused by tissue storage and handling.[18] The refractive power of the isolated lens, free of zonular tension, is also an important input parameter for optical–mechanical finite element models of the lens and accommodation currently in development (Chen J et al. *IOVS* 2006;47:ARVO E-Abstract 5862).[19–21]

The isolated lens power has been shown to decrease with age.[12,13,15,16] A recent study suggests that this decrease is primarily due to age-related changes in the axial profile of the refractive index distribution.[16] The same study suggests that the contribution of the lens surfaces to the total lens power is minor compared with the contribution of the index gradient. On the other hand, Glasser and Campbell[13] found a significant correlation between in vitro lens power and lens surface curvatures, and found no age dependence of the in vitro lens equivalent refractive index. Their findings suggest that there are no significant age-related changes in the contribution of the index gradient to the lens power. A better understanding of the respective contributions from the surfaces and the refractive
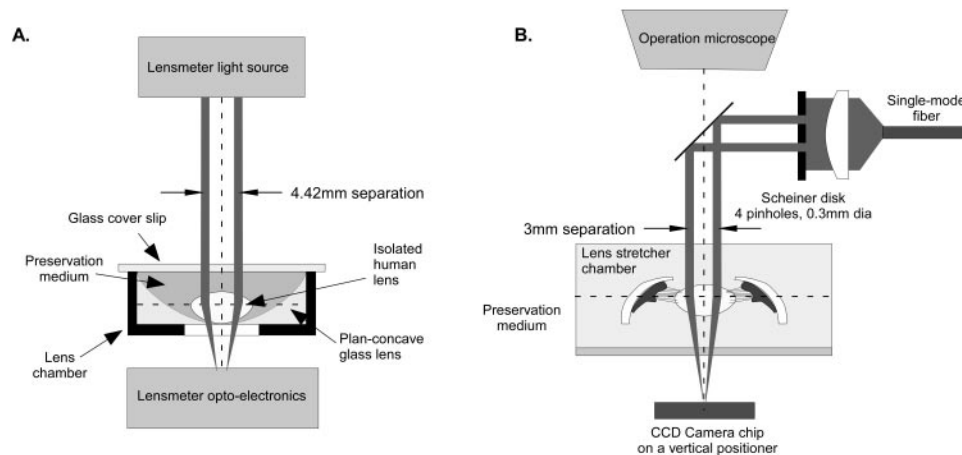
FIGURE 1. (A) Isolated lens refractive power measurement with a commercial lensmeter (Lens Analyzer 350; Carl Zeiss Meditec, Dublin CA). The isolated lens-testing cell consisted of a -20-D plano concave lens (PLCC 01LPK021, $f = -50$ mm, $\varnothing = 40$ mm, $t_c = 2$ mm, Melles Griot, Carlsbad, CA) in a custom-designed lens chamber, filled with DMEM and covered with a glass coverslip (to remove the surface meniscus), giving a total combined optical power of -7 D. (B) In vitro lens power measurement with a Scheiner system.[22] Four parallel beams are directed by a 45° mirror into the vertical direction coaxially with the optical axis of the in vitro lens. A CCD chip mounted on a vertical position is used to visualize and record the location of the focus. In both cases, the anterior of the surface of the lens is up.

index gradient to the in vitro lens power with age will help characterize the optical changes associated with presbyopia.

The purpose of the present study was to characterize the age-dependence of the isolated human crystalline lens power and quantify the contributions of the lens surfaces and refractive index gradient.

MATERIALS AND METHODS

General Description

The power and shape of in vitro human lenses were measured and used to calculate the refractive contributions of the lens surfaces and the gradient refractive index. The lens power data were obtained from two different experiments. In one experiment, the dioptric power of the isolated lens was measured with a modified commercially available lensmeter (Lens Analyzer 350; Carl Zeiss Meditec, Inc., Dublin, CA) (Denham DB et al. *IOVS* 2003;44:ARVO E-Abstract 244). In the other experiment, the dioptric power of lenses maintained in their accommodative framework (with intact zonules, ciliary body, and segmented scleral rim) and mounted in the testing cell of a lens-stretching system (ex vivo accommodation simulator [EVAS]) under no applied tension was measured with a custom designed optical system based on the Scheiner principle.[22] Both systems were calibrated on plano convex glass lenses in the power range of 10 to 45 D. The measurement error ranged from -1.8 to 2.9 D (average, 1.5 D) for the Scheiner system and from 0.32 to 1.47 D (average, 0.61 D) for the commercial lensmeter. In a comparison of the two systems, a Bland-Altman analysis was performed on 14 pairs of crystalline lenses (age: 26–82 years; average age: 54 years) where one eye was measured with the commercial lensmeter and the contralateral eye was measured with the Scheiner system. The mean difference between the two techniques was 1.1 ± 2.2 D with the commercial lensmeter providing the higher average value and no age dependence ($P = 0.374$). This difference is within the expected accuracy and variability of the measurements on in vitro crystalline lenses.

Donor Tissue

All eyes were obtained and used in compliance with the guidelines of the Declaration of Helsinki for research involving the use of human tissue. Experiments were performed on 100 eyes of 73 phakic donors. The donor globes arrived in sealed, Styrofoam containers filled with ice and used between 1 and 5 days postmortem (average, 2.8 ± 1.6 days). The donor ages ranged from 6 to 94 years. Any lens with visible damage or with an equatorial diameter to sagittal thickness aspect ratio less than 2.0 was considered swollen and excluded from the analysis.[18] In total, 24 of the 100 lenses were discarded due to swelling from storage conditions or manipulation during the experiment.

Isolated Lens Power Measurements with a Modified Commercial Lensmeter

For lens power measurements on isolated lenses ($n = 52$), tissue dissection was performed under an operation microscope by an ophthalmic surgeon. First, for stability, a fixed ring was attached to the sclera around the anterior chamber with cyanoacrylate glue. The posterior pole was then sectioned, and the cornea and iris were removed. The lens was then extracted by carefully cutting the zonules and adherent vitreous with Vannas scissors. The isolated lens was immediately immersed in a vial filled with preservation media (DMEM/F-12, D8437; Sigma-Aldrich, St. Louis, MO).[18]

Dioptric power measurements of the isolated lens were performed with a custom modified commercial lensmeter (Lens Analyzer 350; Carl Zeiss Meditec; Fig. 1A). This system delivers four parallel beams arranged in a 4.24-mm square pattern on the test lens. The lens refracts the incident beams and brings them to a focus. An optoelectronic system measures the focus position and calculates lens power. For the measurements, the crystalline lenses were positioned in a custom-designed testing cell filled with preservation medium. The testing cell was designed to offset the optical power of the test lens by -7 D, to increase the measurement range of the lensmeter.

All power measurements on isolated lenses took less than10 minutes.

Mounted Lens Power Measurements with a Scheiner Lensmeter

For the lenses measured in the lens stretcher ($n = 51$) the dissection was performed under an operation microscope by an ophthalmic surgeon. The tissue preparation followed the same protocol as described in a previous study.[22] In this technique a band of eight independent scleral shoes were bonded with cyanoacrylate adhesive (Duro SuperGlue; Henkel Locktite Corp, Cleveland, OH) onto the anterior sclera surface from the limbus to the equator. The band of sclera prevents deformation of the globe during dissection and the shoes
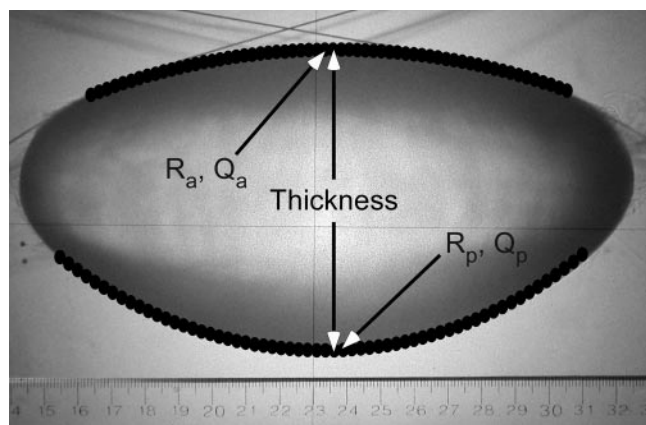
FIGURE 2. A sample sagittal (side view) shadowgraph image of a 53-year-old isolated lens 2 days postmortem, with the anterior and posterior surface profiles overlaid. The surface profiles were fit with conic sections to calculate the anterior and posterior radii of curvature (R_a and R_p) and asphericities (Q_a and Q_p). The thickness was measured directly from the images with a ruler used for calibration. The image shows the crosshairs of the optical comparator and the supporting suture mesh of the immersion cell. During the measurement, the camera was inverted. In this image the lens was photographed with the anterior surface resting on the suture wires.

provide attachment for the lens-stretching device. The posterior pole was then sectioned, and the partially dissected tissue was transferred to the lens-stretching chamber, which was filled with the DMEM preservation medium. Scleral incisions were made between adjacent shoes, and the cornea and iris were removed to produce eight individual segments for stretching. Only the power measured with no tension applied (unstretched state) was used for the present study.

The optical power measurements of the lens while mounted in the lens stretcher system were performed with a custom designed optical system based on the Scheiner principle (Fig. 1B). This system places four parallel laser beams (arranged in a 3-mm square pattern) incident on the lens. The parallel beams are focused by the lens. A camera mounted on a vertical translation stage is positioned at the location of convergence of the four incident beams. This location corresponds to the focal plane of the lens. The dioptric power of the lens immersed in the testing chamber is calculated with a formula derived from a paraxial optical model of the system. On average, the lens was immersed in DMEM for approximately 30 minutes until the power measurements were completed.

When the tissue was not needed for other experiments (11/51 lenses), the lens was extracted by a surgeon at the end of the stretching experiment by carefully cutting the zonules and adherent vitreous with Vannas scissors. The isolated lens was immediately immersed in a DMEM-filled vial to prevent swelling.[18,23] A separate preliminary study had shown that the shape and power of the unstretched crystalline lens are not affected by stretching experiments (Parel JM et al. *IOVS* 2002;43:ARVO E-Abstract 406).

Lens Shape Measurements

On completion of the lens power measurements, the shape of the isolated lens was measured with an optical comparator (model BP-30S; Topcon, Tokyo, Japan).[24] Digital photographs of sagittal views were recorded at 20× magnification in a protocol described previously.[23] During these measurements, the lens was positioned in an immersion chamber filled with DMEM. The lens was supported by a meshwork of 10-0 nylon monofilament sutures. The central lens thicknesses (t), as well as the anterior and posterior surface profiles, were obtained from the shadowgraph images (Fig. 2). The surface profiles were fit with conic functions over the central 6-mm zone, to calculate the radii of curvatures (R) and asphericities (Q).[23,25] In total, the lenses were immersed in preservation medium on average for 20 to 30 minutes for

isolated lenses and 1 to 2 hours for lenses measured in the lens stretcher.

Contributions of Surface Refraction to Total Refractive Power of Isolated Lenses

The refractive contributions of the lens aspheric surfaces were quantified by calculating the power of each measured lens assuming a uniform refractive index equal to the cortex refractive index. Based on the MRI data of Jones et al.,[16] the refractive index of the cortex was assumed to be 1.3709, independent of age. The calculations were performed with commercial optical ray-tracing software (OSLO LT; Lambda Research, Littleton, MA). The ray-tracing simulation incorporates isolated crystalline lens thickness, surface curvature, and asphericity measurements. The refractive index of the surrounding medium (DMEM) was assumed to be equal to the refractive index of water (1.332 at 635 nm). To simulate the experimental conditions, a ray with a height of 1.5 mm (Scheiner) or 2.24 mm (commercial lensmeter) was traced entering the lens. The position of the focal plane was determined by the location of the intersection point of the ray with the optical axis.

Equivalent Refractive Index Calculations

The equivalent refractive index (Neq) is defined as the uniform refractive index value that is required inside the lens to provide a power equal to the actual crystalline lens power if all other parameters (R, Q, and t) remain equal. To calculate the equivalent refractive index for each lens, an optical ray-tracing simulation of the power measurement setups, incorporating the chamber and the measured lens biometric data (lens radii of curvature, asphericities, and thickness) was performed with commercial optical ray-tracing software (OSLO LT; Lambda Research). The refractive index of the simulated lens was adjusted iteratively until the power of the lens corresponded to the measured power.

The technique for calculating the equivalent refractive index was calibrated with a 61-D plano convex glass (SF5; 1.6683) lens, a 36.7-D plano convex glass (BK7; 1.5150) lens, and a 19.2-D plano convex glass (BK7) lens. The shape of the lenses was measured from shadowgraph images, according to the same procedure as that used for the isolated lenses. The refractive index calculated from the measured equivalent power, thickness, diameter, and radius of curvature was within 0.006 to 0.013 of the specified value at 635 nm. An analysis of the sources of error shows that the error in the refractive index comes mainly from the error in the power measurements.
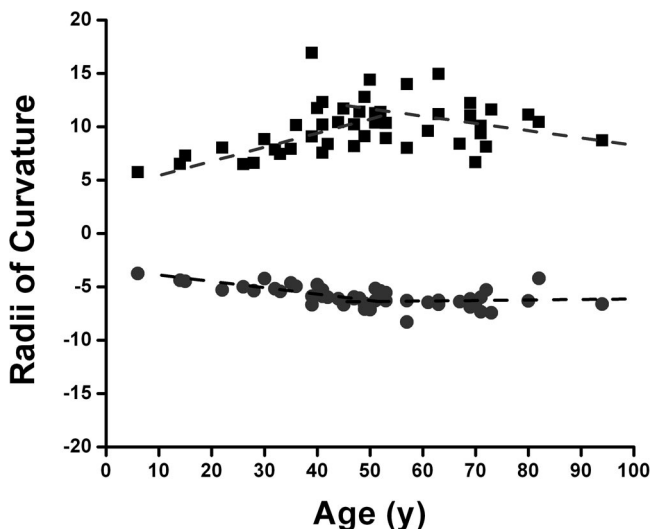

FIGURE 3. In vitro lens anterior ($n = 47$) and posterior radii of curvature ($n = 48$). The equations for the regression lines are given in Table 1.
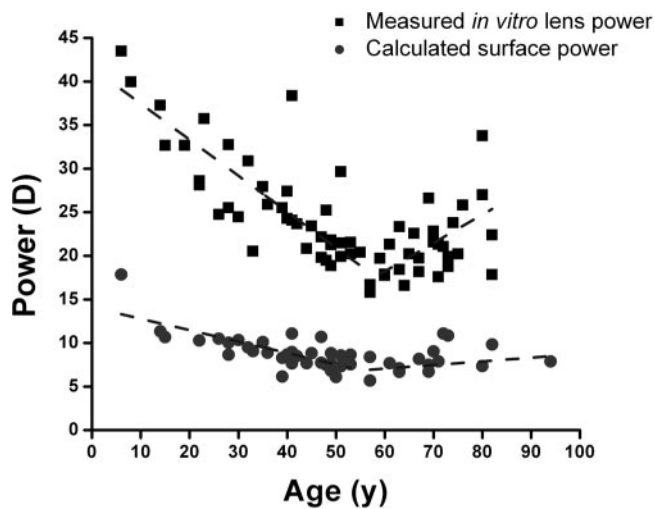
FIGURE 4.   In vitro lens refractive power ($n = 65$) and calculated surface refractive power ($n = 48$). Surface power was calculated from surface curvature measurements obtained during isolated lens biometry. The equations for the regression lines are given in Table 1.

Data and Statistical Analysis

There was a strong correlation between the power and the refractive index of the left and right eye from the same donor. Therefore, to prevent values obtained from paired eyes from skewing the age dependence, the indices from both eyes of each donor were averaged. The average values were then used as a single point for age-dependence calculations. The total power, surface contribution, and equivalent refractive index were plotted as a function of age, to characterize the age dependence. A single or piecewise linear regression was calculated for each data plot, to determine whether there was an age dependence. $P < 0.05$ was set as the condition for statistical significance. For each donor the right and left eye average for each parameter was used as a single data point to characterize age dependence.

RESULTS

Over the age range of the sample set (6–94 years), the age dependence of both total and calculated surface powers, as well as the anterior and posterior surface curvatures, appear to be biphasic, with a change in trend occurring approximately within the period of onset of presbyopia (40–60 years; Figs. 3, 4A; Table 1). Given these apparently biphasic trends, the age dependences for total power, calculated surface power, relative surface contribution, equivalent refractive index, and surface curvatures were analyzed with a bilinear model (Appendix). Applying a nonlinear regression technique to this model, a breakpoint age was identified for each parameter. The breakpoint age divides the data set into two age groups: data points whose age lies below the breakpoint age (which will be referred to as the younger age group throughout this article), and data points whose age lies above the breakpoint age (the older age group). The nonlinear regression outcome on the bilinear model is summarized in Table 2. Predicted anterior and posterior radii of curvatures from the bilinear model are plotted in Figure 3 and the predicted total and calculated surface powers from the bilinear model are plotted in Figure 4.

For both total and surface powers and for anterior and posterior radii of curvature, the bilinear model showed statistical significance ($P < 10^{-5}$) and low SE of estimates (3.76 D for total and 1.5 D for surface power; 2.16 mm for anterior and 0.63 mm for posterior radius). In the younger age group lenses, there was a decrease in total and surface powers, the total power decreasing at a faster rate (-0.41 D/y) than the surface power (-0.13 D/y). In the older age group lenses, total lens power increased at a greater rate ($+0.33$ D/y) than did surface power ($+0.04$ D/y). Anterior and posterior (absolute value) radii of curvature increased in the younger age range at a rate of 0.157 mm/y and 0.058 mm/y and decreased in the older age range at a rate of 0.055 mm/y and 0.027 mm/y, respectively.

There was no statistically significant ($P = 0.74$) breakpoint age for the relative surface refractive contributions (Table 2). There was, however, a statistically significant increase in the relative refractive power contribution from the lens surfaces with age (Fig. 5, Table 1). The surfaces provided from 41% (at 6 years) to 55.1% (at 82 years) of the total refractive power of the isolated lens.

There was a statistically significant ($P < 0.028$) breakpoint age (60.4 years) for the calculated lens equivalent refractive index (Fig. 6, Table 2). In the younger age group, the equivalent refractive index decreased at a rate of -3.88×10^{-4} per year. At the breakpoint age, the equivalent refractive index was

TABLE 1.   Age Dependence of In Vitro Human Lens Optical Properties

	Total Age Range	Lower Age Range	Upper Age Range
Measured equivalent power (D)		$41.59 - 0.41 \cdot$ age (6–58.1 y) $n = 39$	$-1.34 + 0.33 \cdot$ age (58.1–82 y) $n = 26$
Calculated surface power (D)		$14.09 - 0.13 \cdot$ age (6–55.2 y) $n = 33$	$4.58 + 0.04 \cdot$ age (55.2–94 y) $n = 15$
Relative surface refractive contribution (%)*	$30.67 + 0.17 \cdot$ age $P = 0.0031$ $n = 41$	$35.44 + 1.8 \times 10^{-3} \cdot$ age (6–57 y) $n = 29$	$7.37 + 0.49 \cdot$ age (57–82 y) $n = 12$
Equivalent refractive index		$1.4320 - 3.90 \times 10^{-4} \cdot$ age (6–60.4 y) $n = 30$	$1.4096 - 1.82 \times 10^{-5} \cdot$ age (60.4–82 y) $n = 10$
Anterior radius of curvature (mm)		$4.46 + 0.14 \cdot$ age (6–50 y) $n = 26$	$13.83 - 0.05 \cdot$ age (50–94 y) $n = 21$
Posterior radius of curvature (mm)		$-3.47 - 0.06 \cdot$ age (6–57 y) $n = 34$	$-7.97 + 0.02 \cdot$ age (57–94 y) $n = 14$

Data (ages in years) are the in vitro human lens age-dependent linear regression equations of the measured optical properties. The values from both eyes of each donor were averaged and used as a single point for the age-dependence linear regressions.
* The results of the breakpoint analysis were not statistically significant.

TABLE 2. Summary of Statistics for Fitting of a Bi-linear Model against Total Power, Surface Power, Relative Surface Refractive Contribution, Equivalent Refractive Index, and Radii of Curvature versus Age

	Measured Total Power					**Calculated Surface Power**				
Group	**Breakpoint Age (y)**	**Breakpoint Power (D)**	**Direction Cosines (Age, Power)**			**Breakpoint Age (y)**	**Breakpoint Power (D)**	**Direction Cosines (Age, Power)**		
Lower age	58.07	17.60	−0.9242	0.3819		55.26	7.09	−0.9956	0.0941	
Upper age			0.9510	0.3092				0.9991	0.0414	
ANOVA	*df*	**SS**	**MS**	**F**	**Sign**	*df*	**SS**	**MS**	**F**	**Sign**
Model	4	1502.89	375.72	26.61	1.2E-12	4	37.6	9.41	11.14	5.5E-06
Residual	60	847.07	14.12	(SSE = 3.76)		36	30.4	0.9	(SSE = 1.5)	
Total	64	2349.7				40	68.1			

	Relative Surface Refractive Contribution					**Equivalent Refractive Index**				
Group	**Breakpoint Age (y)**	**Breakpoint Value (%)**	**Direction Cosines (Age, %)**			**Breakpoint Age (y)**	**Breakpoint Refractive Index**	**Direction Cosines (Age, Neq)**		
Lower age	57	35.54	−1.00	−0.0018		60.4	1.4085	−1.00	0.0004	
Upper age			0.8932	0.4414				1.00	0.0000	
ANOVA	*df*	**SS**	**MS**	**F**	**Sign**	*df*	**SS**	**MS**	**F**	**Sign**
Model	4	118.29	29.57	0.49	0.741	4	0.0013	0.0003	3.08	0.028
Residual	36	2161.93	60.05	(SSE = 7.75)		35	0.0038	0.0001	(SSE = 0.01)	
Total	40	2280.21				39	0.0051			

	Anterior Radius of Curvature					**Posterior Radius of Curvature**				
Group	**Breakpoint Age (y)**	**Breakpoint Radius (mm)**	**Direction Cosines (Age, Radius)**			**Breakpoint Age (y)**	**Breakpoint Radius (mm)**	**Direction Cosines (Age, Radius)**		
Lower age	49	11.47	0.9879	0.1553		57	−6.75	−0.9983	0.0582	
Upper age			−0.9985	0.0547				0.9999	0.0274	
ANOVA	*df*	**SS**	**MS**	**F**	**Sign**	*df*	**SS**	**MS**	**F**	**Sign**
Model	4	418.04	104.51	22.43	2.3E-09	4	40.39	10.10	25.35	6.4E-10
Residual	36	167.75	4.66	(SSE = 2.16)		35	13.94	0.40	(SSE = 0.63)	
Total	40	585.80				39	54.33			

See Appendix for details.

1.4085. In the older age range the equivalent refractive index remained relatively constant with age.

The equations of the linear regressions are given in Table 1.

DISCUSSION

Several previous studies have shown that the isolated lens power decreases with age. Jones et al.[16] found that the decrease in lens power followed a linear trend over the entire age range of their samples (7–82 years). Our study included a larger number of lenses, particularly in the presbyopic age range. With the larger sample size, we found that the age-related changes in total power of the in vitro lens is biphasic, with the transition occurring around or toward the end of the age range of presbyopia onset. The power initially decreases approximately linearly. After this initial linear decrease, there is a trend for both the total power and the calculated surface power to increase in the older presbyopic lenses. This same trend has been reported by Glasser and Campbell[13] for lenses older than 65 years in a study on 19 isolated human lenses with ages ranging from 5 to 96 years (Fig. 7A). Glasser and Campbell attribute this increase to the inclusion of lenses with early
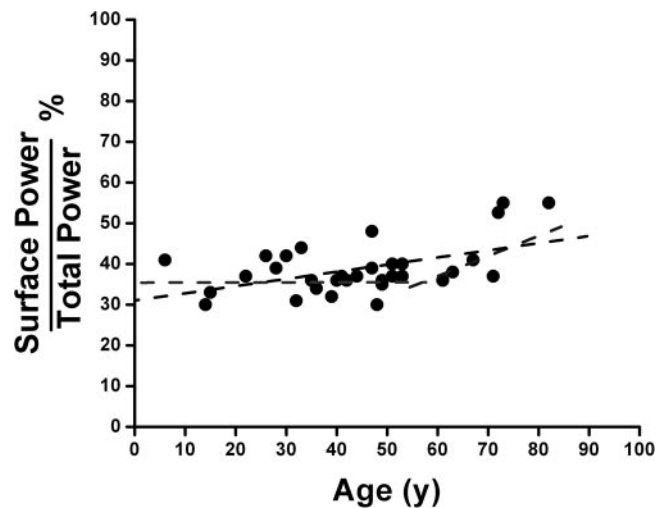

FIGURE 5. The relative surface refractive contributions to the total in vitro lens refractive power as a function of age (*n* = 41). The equation for the regression line is given in Table 1.
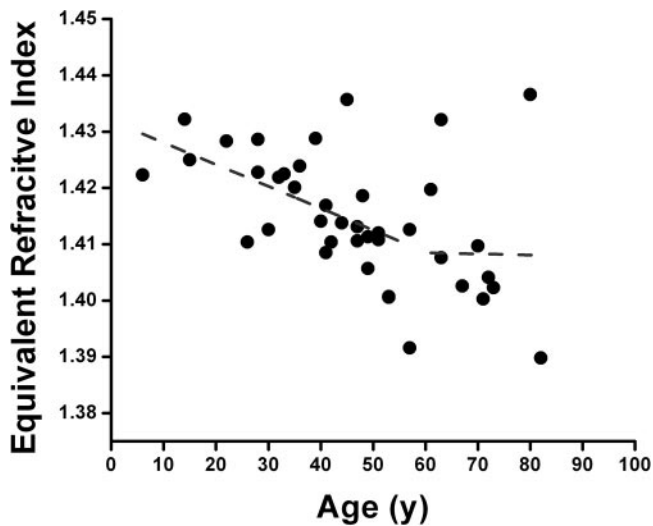
FIGURE 6. The age dependence of the calculated equivalent refractive index of in vitro human lenses ($n = 40$). The equation for the regression line is given in Table 1.

stages of cataract. In our study, 11 of 40 lenses over the age range of 58 to 94 years had some stage of cataract, as evaluated subjectively by grading the color and structure of the lenses in the shadowgraph images. On average, the power and the surface contribution of the cataractous lenses was higher, even though the difference was not statistically significant. This result confirms that the increase in power in older lenses may be due to the effect of cataract formation.

Even though the general trends in our study were similar to those observed by Jones et al.[16] the isolated lens power values that they obtained were significantly higher than our values (by 6.8 D for a 20-year-old lens and by 8.3 D for a 60-year-old lens) as well as the values of Glasser and Campbell[13] (by 7.8 for a 20-year-old lens and by 8.3 D for a 60-year-old lens) and of Schachar.[14] Jones et al.[16] recognized that the lens power in their study was higher than expected. They attributed this difference to a potential increase in lens power beyond maximum accommodation when the lens is removed from the eye. The fact that our results are in excellent agreement with the measurements of Glasser and Campbell,[13] as well as with in vivo measurements,[2,26–31] suggests that the values obtained by Jones et al.[16] overestimated the power of the isolated lens. Our findings show that removing zonular tension does not increase the power of the lens significantly compared with the maximally accommodated in situ lens.

According to our results, the dioptric contribution of the lens surfaces to the total lens power decreases only slightly with age. The decrease of the in vitro lens power with age is

therefore, due mainly to changes of the internal structure of the lens including the cortex. These findings confirm the results of Jones et al.[16] In absolute values the contribution of the surfaces in the present study is similar to their value ($\sim$10 D). The relative contribution (in percent) of the surfaces in our study is higher, as expected since their values seem to overestimate total lens power. We find that the surface refractive contribution increases with age from 26% to 55% of the total lens power (Table 1).

The contribution of the gradient refractive index of the lens to the total lens power is often quantified using the concept of an equivalent refractive index. In a longitudinal study of school age children, Mutti et al.[6] showed that the equivalent refractive index between 5 and 16 years of age is approximately constant, with an average value of 1.427. Dubbelman and Van der Heijde[32] found that the equivalent refractive index decreases with age in the adult eye with values ranging from approximately 1.441 to 1.418 in the age range of 16 to 65 years. Glasser and Campbell[12,13] calculated the equivalent refractive index of isolated lenses from ray-tracing experiments. They did not find a change with age. Their mean equivalent refractive index was 1.4257 ± 0.0163.[13] Glasser and Campbell may not have been able to find an age dependence in equivalent refractive index because of their smaller sample size ($n = 19$). We find that the equivalent refractive index decreases with age from a maximum of 1.437 for a 14-year-old lens to a minimum of 1.396 for an 82-year-old lens.

Our results show the same trend, with a similar decay rate was found by Dubbelman and Van der Heijde[32] (Fig. 7B), but our values are slightly lower. The difference could be due to our measuring the ex vivo lens, which is expected to correspond to the maximally accommodated state, whereas Dubbelman and Van der Heijde[32] measured the refractive index of the relaxed unaccommodated lens in vivo. However, Dubbelman et al.[17] found that the equivalent refractive index slightly increases with accommodation. If the difference is due to a change in accommodative state, then our values should be higher. Most likely, the difference is due to differences in methodology. In our study, we calculated the refractive index of the lens from direct measurements of the lens power and high-resolution measurements of the lens shape, including lens asphericity. Even though in vitro lenses allow direct measurement, they are subject to alterations in lens shape caused by storage and handling. On the other hand, accurate in vivo measurements of the lens equivalent refractive index are difficult to obtain because of the uncertainty of the shape of the posterior lens surface, which is imaged through the internal structure of the lens.[17,32] Despite these potential sources of error in both in vitro and in vivo measurements, there is good agreement between our ex vivo results and the in vivo measurements of Dubbelman and Van der Heijde.[32]
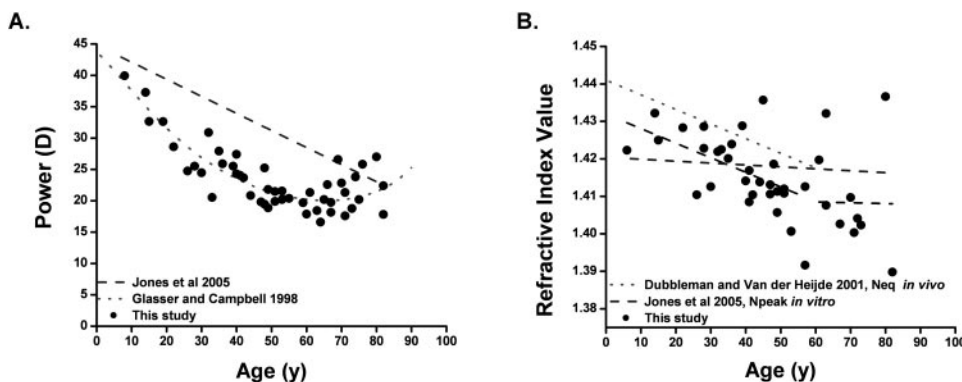

FIGURE 7. Comparison of our results with previously published data on the age dependence of the lens power (**A**) and the refractive index (**B**).
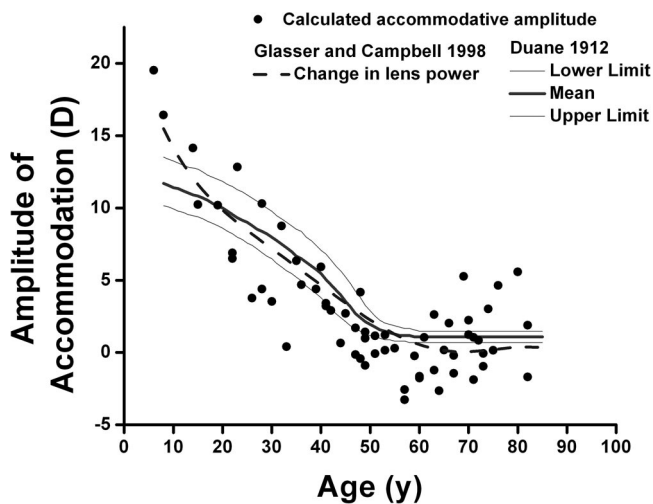
FIGURE 8. Calculated maximum possible accommodative amplitude of each measured lens power data point ($n = 65$). The age-dependent data for the in vivo amplitude of accommodation from Duane[33] (corrected to place the reference plane at the anterior corneal surface instead of the spectacle plane) is superimposed on the graph. There is good agreement between the age-dependent loss of accommodation and the maximum amplitude of accommodation calculated from the isolated lens power.

Our results demonstrate a biphasic age-dependent trend for both anterior and posterior radii of curvatures, which confirms the findings in two studies.[9,13] Since power and radii of curvature exhibit a biphasic age-dependency, we expect to find the same trend in the equivalent refractive index and in the relative contribution of the surfaces to the lens power. There is a statistically significant breakpoint in the equivalent refractive index, but not in the relative contribution of the surface power. A larger sample is needed in the older age range (>55 years), to demonstrate the biphasic trend of these two parameters with a higher confidence level.

Like Glasser and Campbell[12,13] we find that the decrease of in vitro lens power matches well with the decrease of in vivo accommodation amplitude.[33] This result is expected, since it is assumed that the power of the lens when accommodation is relaxed remains approximately constant with age in the adult,[1,28] and the isolated lens is expected to correspond approximately to the maximally accommodated state. The decrease in accommodation amplitude in the adult must therefore correspond directly to a decrease in the power of the maximally accommodated lens (Fig. 8). The relation between in vitro lens power and in vivo accommodation amplitude may not hold in children because there is evidence that the unaccommodated lens power decreases with age in children.[27,30,31,34]

In summary, our measurements are consistent with the findings of Dubbelman et al.[17,32] and of Jones et al.,[16] that there is a decrease in the equivalent refractive index with age or, in other words, the contribution of the gradient refractive index distribution decreases. One of the implications of the decrease in equivalent refractive index with age is that the use of fixed equivalent refractive index value to calculate lens power using the lensmaker formula will underestimate the power of young lenses and overestimate the power of old lenses. Furthermore, an error maybe induced in central lens thickness and posterior radius of curvature calculations when a fixed equivalent refractive index is used[3,35] during analysis of in vivo phakometry or Scheimpflug images. Our measurements confirm that the power and shape of the in vitro lens correspond to that of the in vivo maximally accommodated lens.

References

1. Atchison DA, Smith G. *Optics of the Human Eye*. Boston: Butterworth Heinemann; 2000.
2. Mutti D, Zadnik K, Adams A. A video technique for phakometry of the human crystalline lens. *Invest Ophthalmol Vis Sci*. 1992;33(5):1771–1782.
3. Garner LF. Calculation of the radii of curvature of the crystalline lens surfaces. *Ophthalmic Physiol Opt*. 1997;17(1):75–80.
4. Bennett AG, Rabbetts RB. *Clinical Visual Optics*. 3rd ed. Butterworth-Heinemann; 1998:211–399.
5. Bennett AG. A method of determining the equivalent powers of the eye and its crystalline lens without resort to phakometry. *Ophthalmic Physiol Opt*. 1988;8(1):53–59.
6. Mutti D, Zadnik K, Adams A. The equivalent refractive index of the crystalline lens in childhood. *Vision Res*. 1995;35(11):1565–1573.
7. Koretz JE, Strenk SA, Strenk LM, Semmlow JL. Scheimpflug and high-resolution magnetic resonance imaging of the anterior segment: a comparative study. *J Opt Soc Am A*. 2004;21(3):346–354.
8. Rosales P, Dubbelman M, Marcos S, van der Heijde R. Crystalline lens radii of curvature from Purkinje and Scheimpflug imaging. *J Vision*. 2006;6(10):1057–1067.
9. Howcroft MJ, Parker JA. Aspheric curvatures for the human lens. *Vision Res*. 1977;17(10):1217–1223.
10. Sivak JG, Kreuzer RO. Spherical aberration of the crystalline lens. *Vision Res*. 1983;23(1):59–70.
11. Pierscionek BK, Chan DY. Refractive index gradient of human lenses. *Optom Vis Sci*. 1989;66(12):822–829.
12. Glasser A, Campbell MC. Presbyopia and the optical changes in the human crystalline lens with age. *Vision Res*. 1998;38:209–229.
13. Glasser A, Campbell MCW. Biometric, optical and physical changes in the isolated human crystalline lens with age in relation to presbyopia. *Vision Res*. 1999;39:1991–2015.
14. Schachar RA. Central surface curvatures of postmortem-extracted intact human crystalline lenses: implications for understanding the mechanism of accommodation. *Ophthalmology*. 2004;111(9):1699–1704.
15. Moffat BA, Atchison DA, Pope JM. Age-related changes in refractive index distribution and power of the human lens as measured by magnetic resonance micro-imaging in vitro. *Vision Res*. 2002;42:1683–1693.
16. Jones CE, Atchison DA, Meder R, Pope JM. Refractive index distribution and optical properties of the isolated human lens measured using magnetic resonance imaging (MRI). *Vision Res*. 2005;45(18):2352–2366.
17. Dubbelman M, Van der Heijde GL, Weeber HA. Change in shape of the aging human crystalline lens with accommodation. *Vision Res*. 2005;45:117–132.
18. Augusteyn RC, Rosen AM, Borja D, Ziebarth NM, Parel JM. Biometry of primate lenses during immersion in preservation media. *Mol Vis*. 2006;12:740–747.
19. Burd HJ, Judge SJ, Cross JA. Numerical modelling of the accommodating lens. *Vision Res*. 2002;42(18):2235–2251.
20. Schachar RA, Abolmaali A, Le T. Insights into the age-related decline in the amplitude of accommodation of the human lens

using a non-linear finite-element model. *Br J Ophthalmol.* 2006; 90(10):1304–1309.

21. Hermans EA, Dubbelman M, van der Heijde GL, Heethaar RM. Estimating the external force acting on the human eye lens during accommodation by finite element modelling. *Vision Res.* 2006;46: 3642–3650.

22. Manns F, Parel JM, Denham D, et al. Optomechanical response of human and monkey lenses in a lens stretcher. *Invest Ophthalmol Vis Sci.* 2007;48(7):3260–3268.

23. Rosen AM, Denham DB, Fernandez V, et al. In vitro dimensions and curvatures of human lenses. *Vision Res.* 2006;46:1002–1009.

24. Denham D, Holland S, Mandelbaum S, Pflugfelder S, Parel JM. Shadow photogrammetric apparatus for the quantitative evaluation of corneal buttons. *Ophthalmic Surg.* 1989;20:794–799.

25. Manns F, Fernandez V, Zipper S, et al. Radius of curvature and asphericity of the anterior and posterior surface of human cadaver crystalline lenses. *Exp Eye Res.* 2004;78(1):39–51.

26. Garner LF, Yap M, Scott R. Crystalline lens power in myopia. *Optom Vis Sci.* 1992;69(11):863–865.

27. Zadnik K, Mutti DO, Friedman NE, Adams AJ. Initial cross-sectional results from the Orinda Longitudinal Study of Myopia. *Optom Vis Sci.* 1993;70(9):750–758.

28. Hemenger RP, Garner LF, Ooi CS. Change with age of the refractive index gradient of the human ocular lens. *Invest Ophthalmol Vis Sci.* 1995;36(3):703–707.

29. Goss DA, Van Veen HG, Rainey BB, Feng B. Ocular components measured by keratometry, phakometry, and ultrasonography in emmetropic and myopic optometry students. *Optom Vis Sci.* 1997; 74(7):489–495.

30. Jones LA, Mitchell GL, Mutti DO, et al. Comparison of ocular component growth curves among refractive error groups in children. *Invest Ophthalmol Vis Sci.* 2005;46(7):2317–2327.

31. Ip JM, Huynh SC, Kifley A, et al. Variation of the contribution from axial length and other oculometric parameters to refraction by age and ethnicity. *Invest Ophthalmol Vis Sci.* 2007;48(10):4846–4853.

32. Dubbelman M, Van der Heijde GL. The shape of the aging human lens: curvature, equivalent refractive index and the lens paradox. *Vision Res.* 2001;41:1867–1877.

33. Duane A. Normal values of the accommodation at all ages. *JAMA.* 1912;59:1010–1013.

34. Mutti DO, Mitchell GL, Jones LA, et al. Axial growth and changes in lenticular and corneal power during emmetropization in infants. *Invest Ophthalmol Vis Sci.* 2005;46(9):3074–3080.

35. Garner LF, Yap MK. Changes in ocular dimensions and refraction with accommodation. *Ophthalmic Physiol Opt.* 1997;17(1):12–17.

APPENDIX

Fitting of a Bilinear Model to an Apparently Biphasic Data Set by Using an Iterative Computational (Nonlinear Regression) Technique

Given the apparent biphasic nature of the relationships for measured total power and calculated surface power versus age, we tested the data set against a bilinear model. Mathematically, the bilinear model can be represented (given here in parametric column–matrix form, as it best illustrates the concept) by:

$$
\begin{bmatrix} X \\ Y' \end{bmatrix} = \begin{cases} \begin{bmatrix} X_{bp} \\ Y_{bp} \end{bmatrix} + k_L \cdot \begin{bmatrix} L_x \\ L_y \end{bmatrix} & \text{for } X \le X_{bp} \\ \begin{bmatrix} X_{bp} \\ Y_{bp} \end{bmatrix} + k_U \cdot \begin{bmatrix} U_x \\ U_y \end{bmatrix} & \text{for } X > X_{bp} \end{cases}
$$

where X is the x value (age); Y' is the predicted y value (total power, calculated surface power); X_{bp} is the breakpoint age; Y_{bp} is the predicted y value at the breakpoint age; k_L and k_U are scalar parameters; L_x, and L_y are direction cosines for points with age below breakpoint age; and U_x, and U_y are direction cosines for points with age above breakpoint age.

It can be seen from the equation that conceptually, the bilinear model defines a breakpoint age value that divides the data set into two subsets; one subset of data points with ages lying below the breakpoint age and a second subset with ages lying above the breakpoint age. A line of best fit is then found for each of the two subsets, with the additional constraint that the two lines intersect at the breakpoint (X_{bp}, Y_{bp}).

Values for the best fitting (X_{bp}, Y_{bp}), (L_x, L_y), and (U_x, U_y) are found by the least-squares method (minimizing the total sum of squares of residuals for both subsets of data combined). The computations were achieved with commercial software (Solver tool in Excel, ver. 2003; Microsoft, Redmond, WA). The results are given in Table 2.

In consideration of the degrees of freedom in this regression model, although the above equation is written with six variables, effectively, the model involves the fitting of two lines, each with its independent slope and intercept. Once these two lines are defined, their intersection defines, without further degrees of freedom, the breakpoint. Hence, a total of 4 degrees of freedom are assignable to this model and used for the *F*-test analyses in Table 2.